Machine Learning for Rectangular Waveguide Mode Identification, Using 2D Modal Field Patterns

SUBMISSION DATE / POSTED DATE

10-10-2022 / 14-10-2022

DOI

10.36227/techrxiv.21307800.v1

Machine Learning for Rectangular Waveguide Mode-Identification, Using 2D Modal Field Patterns

Brian Guiana and Ata Zadehgol
Department of Electrical and Computer Engineering, University of Idaho, Moscow, ID 83844–1023
Email: bguiana@uidaho.edu and azadehgol@uidaho.edu

***Abstract*—We apply machine learning (ML) techniques to identify the modes in rectangular waveguides from images of 2D modal field patterns injected with uniform, exponential, correlated exponential, and Gaussian noise distributions. A binary classifier is used to identify either transverse electric (TE) or transverse magnetic (TM) modes, and a Multi-class classifier is used to identify the mode numbers. Signal to noise ratios of 1, 0.1, and 0.01 are used to show the effectiveness of each model. Results show accuracy scores up to 99.95%. Several examples demonstrate that noisy modal patterns (unidentifiable to human eyes) may be successfully classified by the ML model.**

I. Introduction

Rectangular waveguides (RWG) are commonly used in electromagnetic applications [1]–[3]. In a RWG with perfect electric conductor (PEC) boundaries, analytical expressions [1], [2] may be used to obtain the cross-sectional frequency-domain field components; conversely, given an image of a 2D modal field pattern (magnitude and phase), with minimal effort one may use the analytical expressions to determine the modal information; i.e., $\text{TE}_{m,n}$ or $\text{TM}_{m,n}$, and mode numbers $\{m, n\} \in$ Integers. However, if noise (due to measurement or modeling errors) is added to the image, then the mode-identification via simple (human) visual inspection may not be feasible; e.g., Fig 3(c)-(d). We show that although modal-identification by ML model becomes challenging for small *signal-to-noise ratio (SNR)*, it still outperforms detection by visual inspection. In this paper, the modal field patterns are modulated by random noise sources which are applied as *correlated* and *uncorrelated* [4] noise to data from analytical field components. We employ the *Scikit-Learn* [5] and Python [6] packages and apply methods outlined in [7] to test the ML classification models (MLCM).

II. Methodology and Formulation

We classify RWG modes into TE and TM modes using a binary classifier, and identify mode numbers $\{m, n\}$ with a multi-class classifier. We use the *K-Neighbors* classification model here, as it was shown to function well in [8] for MNIST image recognition, where the binary classifier has two output classes (or levels) and the multi-class classifier has ten output levels. We use the *distance* option with four neighbors for the classifier, placing weight on surrounding pixels inverse proportionally to the distance from other pixels. Our experiments assume typical K-band rectangular waveguides composed of PEC sidewalls surrounding a good dielectric core ($\epsilon_r \approx 4.0$, $\sigma = 0$ (S/m), and $\mu = \mu_0$ (H/m)) width $a = 1.07$ cm, height $b = 0.43$ cm, and source frequency $f = 60$ GHz. This setup allows modes above the fundamental to propagate without loss through the waveguide, where the modes are limited to TE_{mn} and TM_{mn} with $0 \leq m, n \leq 3$, excluding $m = n = 0$. Assuming the field components are transverse to $\hat{z}$, the resulting boundary value problem has analytical solutions for all field components in each mode which may be found in Table 3.2 in [1, Ch. 3].

A. Noise Figures

We use three uncorrelated noise distributions and one exponentially correlated noise distribution. Each of these are described by their respective *probability density function (PDF)*. The uncorrelated noise images use uniform, exponential, or Gaussian PDFs. The correlated noise images are generated using the exponential PDF and correlation techniques in [9], where the noise images are two dimensional (2D). Correlation and spectral data for uncorrelated versus correlated noise images are shown in Fig. 1.

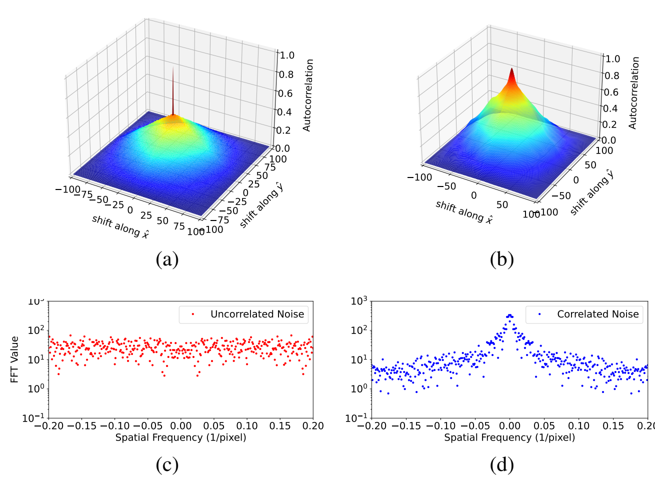

(a) (b)

(c) (d)

Fig. 1: (a) Uncorrelated and (b) correlated noise autocorrelation; (c) uncorrelated and (d) correlated noise spectrum.

The correlated noise images are generated automatically with the Pyspeckle package [9]. The control image (with no noise) and examples of noisy images are shown in Fig. 2, where values have been normalized to be in $[0, 1]$.

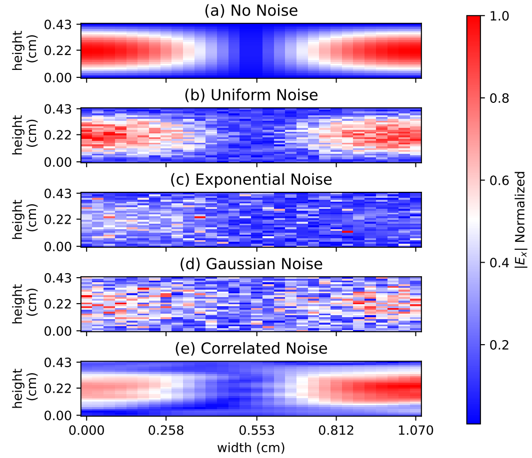

Fig. 2: Magnitude of E_x in the TE_{11} mode with each noise figure at SNR=1.

III. Results and Discussion

A. Data Generation and Selection

We use the E_x and E_y field components with a 30×30 pixel resolution. One noisy image is generated for each real and imaginary component of E_x and E_y (4 total per sample), and each image is injected to have SNR$=\{1, 0.1, 0.01\}$, where smaller SNR values indicate more noise than signal. 10,000 samples were generated with random modes for each corner plus a noiseless control (130,000 samples total). Magnitude plots of E_x for each of the noise images at SNR=1 are shown in Fig. 2, and the correlated noise images are shown at each SNR target in Fig. 3.

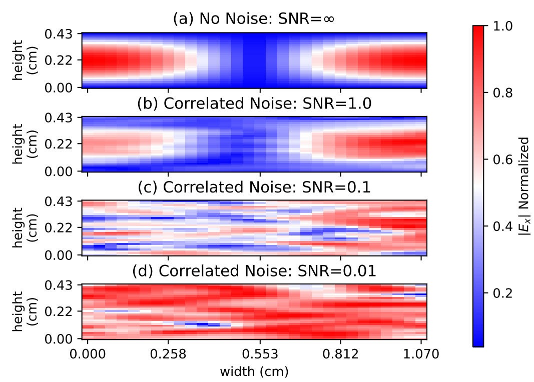

Fig. 3: Magnitude of E_x in the TE_{11} mode with correlated noise figure at each SNR.

B. Training and Testing Classification Models

The accuracy scores are shown in Table I, where a score of 1.0 indicates perfect detection, and where a score of 0.5 for the binary classifier and 0.1 for the multi-class classifier indicates random guessing. The control and the SNR=1 results show a perfect score, and the results at SNR=0.01 show random guessing for both models. For example, with the binary classifier we find the order of *goodness* with SNR=0.1 is (1) uniform, (2) exponential, (3) correlated, and (4) Gaussian noise, where uniform noise is almost ignored, Gaussian noise causes nearly random guessing, and the uncorrelated and correlated exponential noise images show scores nearly uniformly spaced between random guessing and perfect scores. The order

TABLE I: Accuracy Scores of Classification Models

	Binary Classifier			Multi-class Classifier		
SNR	1.0	0.1	0.01	1.0	0.1	0.01
Control	1.0	N/A	N/A	1.0	N/A	N/A
Uniform Noise	1.0	0.9985	0.4885	1.0	0.9995	0.1165
Exponential Noise	1.0	0.8150	0.5050	1.0	0.7055	0.1190
Gaussian Noise	1.0	0.5470	0.5085	1.0	0.2080	0.1135
Correlated Noise	1.0	0.6540	0.4970	1.0	0.4240	0.1175

of goodness could be the result of spectral composition in the noise images. The K-neighbors classifier acts as a low-pass filter (for noise), so low-frequency noise is more likely passed through. Correlated noise has increased low-frequency content, so we can expect the uncorrelated exponential noise to outperform its correlated counterpart. However, the spectral content of white noise should be nearly uniform across all frequencies, thus further investigation may be necessary.

IV. Conclusion

Machine learning models based on K-neighbors were trained and tested on RWG modal images with noise injected at three different SNR levels. The results at SNR = 0.1 showed that overall MLCM performance was poor for Gaussian noise, marginally improved for correlated exponential noise, further improved for uncorrelated exponential noise, and was almost unaffected by uniform noise. Increasing the noise by two orders-of-magnitude with SNR=0.01, the MLCM accuracy was much worse. These SNRs were chosen for emphasis, but it may not be common to see SNR< 0.1 in a laboratory environment. This means that for SNR ≥ 0.1, the machine learning model can likely outperform simple visual identification of RWG modes based on images of 2D modal field patterns.

Acknowledgment

This work was funded, in part, by the National Science Foundation [10].

References

[1] D. M. Pozar. *Microwave Electronics*. Wiley, USA, 4th edition, 2012.
[2] C. A. Balanis. *Advanced Engineering Electromagnetics*. Wiley, USA, 1st edition, 1989.
[3] Brian Guiana and Ata Zadehgol. Characterizing THz Scattering Loss in Nano-Scale SOI Waveguides Exhibiting Stochastic Surface Roughness with Exponential Autocorrelation. *Electronics*, 11(3), 2022.
[4] D Duncan and Sean Kirkpatrick. Algorithms for simulation of speckle (laser and otherwise). 01 2008.
[5] scikit-learn. https://scikit-learn.org/stable/. Accessed: June 13, 2022.
[6] Python. https://www.python.org/. Accessed: June 13, 2022.
[7] Aurélien Géron. *Hands-On Machine Learning with Scikit-Learn, Keras, & TensorFlow*. O'Reilly Media, Inc., Second edition, Sept. 2019.
[8] Aurélien Géron et al. handson-ml2. [Online] github.com/ageron/handson-ml2/. Accessed: 10 Feb. 2022.
[9] Pyspeckle. https://pyspeckle2.readthedocs.io/en/latest/#. Accessed: Oct. 15, 2021.
[10] Ata Zadehgol. SHF: SMALL: A novel algorithm for automated synthesis of passive, causal, and stable models for optical interconnects. National Science Foundation (NSF) Award #1816542.